

# Modification of the Charge ordering in $\text{Pr}_{1/2}\text{Sr}_{1/2}\text{MnO}_3$ Nanoparticles

Anis Biswas, I. Das and Chandan Majumdar

*Saha Institute of Nuclear Physics, 1/AF,  
Bidhannagar, Kolkata 7000 064, India*

## Abstract

Transport and magnetic properties have been studied in two sets of sol-gel prepared  $\text{Pr}_{1/2}\text{Sr}_{1/2}\text{MnO}_3$  nanoparticles having average particle size of 30 nm and 45 nm. Our measurements suggest that the formation of charge ordered state is largely affected due to lowering of particle size, but the ferromagnetic transition temperature ( $T_C$ ) remains unaffected.

PACS numbers: 75.47.Lx, 73.63.Bd

## I. INTRODUCTION

Interests have grown recently towards the study of hole doped Perovskite Manganites with general formula  $R_{1-x}A_xMnO_3$  (R - Trivalent Rare earth, A - Bivalent ions) because they exhibit intriguing phenomena like Colossal Magnetoresistance (CMR), Charge ordering (CO) etc.<sup>1,2</sup>. Charge ordering is observed for commensurate fraction of concentration of bivalent ion such as  $1/8$ ,  $1/3$  and  $1/2$ <sup>1,2</sup>. This phenomenon draws considerable attention because it exhibits a close interrelation among magnetic ordering, electronic transport and crystal structure. Large magnetoresistance (MR) also originates due to the melting of CO state by magnetic field<sup>3</sup>. There are several reports on this phenomena in the  $x \sim 1/2$  systems like  $Nd_{1-x}Sr_xMnO_3$ <sup>4</sup>,  $La_{1-x}Ca_xMnO_3$ <sup>5,6</sup>,  $Pr_{1-x}Ca_xMnO_3$ <sup>7,8,9,10</sup>,  $Pr_{1-x}Sr_xMnO_3$ <sup>11,12,13</sup>. Most of the above mentioned materials exhibit C-E type charge ordering. However, very few of them with relatively large single electron band-width show stripe like A-type antiferromagnetic charge ordering. As the A-type antiferromagnets are made of alternately stacked ferromagnetic planes, the ferromagnetism and antiferromagnetism are closely connected in such systems. Therefore, the materials exhibiting A-type antiferromagnetic charge ordering offer an opportunity to study the competition of ferromagnetic double exchange interaction and antiferromagnetic super exchange interaction in charge ordered lattice. In case of single crystalline form of  $Pr_{1/2}Sr_{1/2}MnO_3$  two transitions occur. During cooling from 300 K it undergoes paramagnetic to ferromagnetic state at  $\sim 270$  K and then ferromagnetic to charge ordered antiferromagnetic state at  $\sim 140$  K<sup>12</sup>. Insulator to metal transition also occurs in coincidence with the paramagnetic to ferromagnetic transition at  $\sim 270$  K and resistivity starts to increase sharply with decreasing temperature below  $\sim 140$  K due to the charge order transition<sup>12</sup>. Recently, through neutron diffraction study it has been conclusively proved that in this sample the charge ordering is not conventional checker board type (C-E type); it is novel stripe like A-type antiferromagnetic<sup>13</sup>. The detection of this novel kind of charge ordering may not be straightforward and it has not been clearly detected in earlier neutron diffraction study<sup>14</sup>. Though there are considerable studies in the single crystalline and polycrystalline bulk form of  $Pr_{1/2}Sr_{1/2}MnO_3$  regarding charge ordering, but this phenomena is not explored much in its nanocrystalline form. In this report, our primary objective is to study the modification of the charge ordering in case of the nanoparticles of  $Pr_{1/2}Sr_{1/2}MnO_3$ . With this motivation, the nanoparticles of  $Pr_{1/2}Sr_{1/2}MnO_3$  have been synthesized by sol-gel

method. Since charge ordering in single crystalline form of  $\text{Pr}_{1/2}\text{Sr}_{1/2}\text{MnO}_3$  has strong signature in transport and magnetic properties, we have performed transport, magnetotransport and magnetization measurements in details to study the charge ordering in case of the above mentioned nanoparticles. From our measurements, it appears that the formation of CO state is hindered due to the lowering of grain size and the transition from ferromagnetic state to antiferromagnetic CO state is not clearly evident. However, the ferromagnetic transition temperature remains unaffected.

## II. SAMPLE PREPARATION AND CHARACTERIZATION

Nanoparticles of  $\text{Pr}_{1/2}\text{Sr}_{1/2}\text{MnO}_3$  have been prepared by sol-gel method. The starting materials are  $\text{Pr}_6\text{O}_{11}$ ,  $\text{MnO}_2$  and  $\text{SrNO}_3$  with the purity of 99.9 %. The oxides have been converted to nitrates and suitable amount of citric acid is mixed with the water solution of the nitrates. Then the solution has been slowly evaporated until a gel is formed. The gel is decomposed into a black porous powder. This porous powder is then divided into several parts, which are kept under heat treatment at different temperatures to prepare samples of different particle sizes. Powder X-ray diffraction pattern (XRD) shows that single phased sample is formed when sample is heated at temperature  $1200^\circ\text{C}$  and above. Two sets of sample of different particle sizes have been prepared by heat-treatment for 4 hours at  $1200^\circ\text{C}$  and  $1400^\circ\text{C}$  respectively. From the Transmission Electron Microscopy measurements, average particle sizes are determined as 30 nm and 45 nm for  $1200^\circ\text{C}$  and  $1400^\circ\text{C}$  heat treated samples. To compare the results of nanocrystalline samples with polycrystalline bulk sample, we have also prepared polycrystalline bulk form of  $\text{Pr}_{1/2}\text{Sr}_{1/2}\text{MnO}_3$  by solid state reaction from the stoichiometric ratio of  $\text{Pr}_6\text{O}_{11}$ ,  $\text{MnO}_2$  and  $\text{SrCO}_3$ . In this case, after several intermediate heat treatments at  $1000^\circ\text{C}$ , final heat treatment has been given at  $1500^\circ\text{C}$  for 22 hours. The XRD pattern confirms the single phase nature of the sample in this case also.

## III. EXPERIMENTAL RESULTS AND DISCUSSION

The resistivity measurements have been performed in usual four probe method. The temperature dependence of resistivity in the temperature range 3.3 K - 300 K for the poly-

crystalline bulk  $\text{Pr}_{1/2}\text{Sr}_{1/2}\text{MnO}_3$  sample (Fig. 1) shows that there is an insulator to metal transition (I-M) at around 275 K. As temperature is decreased further, resistivity starts to increase sharply below  $\sim 130$  K. These two temperatures are in good agreement with the reported temperatures where I-M transition (paramagnetic to ferromagnetic) and the charge order transition are observed for single crystalline form of the sample<sup>12</sup>. The sharp increase of resistivity with temperature below  $\sim 130$  K is believed to be due to charge order transition.

A commercial SQUID magnetometer has been employed for magnetization measurements. The zero field cooled (ZFC) DC susceptibility with temperature has been studied in presence of 20 kOe magnetic field. The temperature dependence of DC susceptibility for the polycrystalline bulk sample indicates that the paramagnetic to ferromagnetic transition occurs at  $\sim 275$  K where the I-M transition in resistivity measurement is observed. There is also a ferromagnetic to antiferromagnetic transition at around 115 K (Fig. 2) which is slightly lower than the temperature at which resistivity starts to increase sharply with the lowering of temperature (Fig. 1). The transition temperatures are assigned as the temperatures where the fastest change of magnetization with temperature takes place. For the bulk sample, the magnetic field dependence of magnetization is linear at 350 K indicating paramagnetic behavior. The ferromagnetic state in the temperature range between 275 K and 115 K has been confirmed by  $M(H)$  measurements at 225 K (Fig. 3). The  $M(H)$  measurements at 3.3 K also confirms the antiferromagnetic state below 115 K (Fig. 3). For the bulk sample, an abrupt increase of magnetization occurs at around 55 kOe in  $M(H)$  data at 3.3 K (Fig. 3). It can be attributed to the metamagnetic transition due to melting of CO state by magnetic field. An appreciable hysteresis is also observed in  $M(H)$ . The polycrystalline bulk sample shows all the features and transition temperatures of  $\text{Pr}_{1/2}\text{Sr}_{1/2}\text{MnO}_3$  which are consistent with the literature<sup>12</sup> and the results of the sample can be used to compare with the results obtained for nanocrystalline samples.

The study of variation of resistivity with temperature for nanoparticles of different sizes (Fig. 1) reveals that there is no indication of I-M transition in the entire temperature range (3.3 - 300 K). Instead of this resistivity increases with the decrease of temperature down to 3.3 K. This increase is reasonably fast in the low temperature region. But the increase of resistivity is not as sharp as in the case of polycrystalline sample. From the temperature dependence of resistivity for nanocrystalline samples, it is quite difficult to comment whether

the increase of resistivity are connected with charge ordering or some other effect.

The temperature dependence of ZFC susceptibility for nanoparticles shows a transition from paramagnetic to ferromagnetic state at around 275 K which is also  $T_C$  for bulk sample (Fig. 2). However, ferromagnetic to antiferromagnetic transition is not evident for both the nanocrystalline samples. The ZFC susceptibility measurement has been carried out in the presence of 20 kOe magnetic field. For both the samples,  $M(H)$  behavior at 350 K is linear confirming the paramagnetic state of the samples. There is a decrease in the rate of change of magnetization from temperature around 140 K in comparison to the higher temperature region. It appears that the value of susceptibility for 45 nm particle sized sample is larger than that for other nanocrystalline sample in temperature region above  $\sim 140$  K and below this temperature susceptibility of 30 nm sample is larger than that of 45 nm sample. We further study the variation of field cooled (FC) and zero field cooled susceptibility with temperature in the presence of 100 Oe magnetic field for the nanocrystalline samples. The FC and ZFC susceptibility curve for the sample of particle size 45 nm has been shown in Fig. 4. A large bifurcation between ZFC and FC susceptibility has been observed below  $T_C$ . Usually nanoparticles can be considered to be composed of two parts. The inner part is core and the outer part is grain boundary or surface layer. The surface layers are in disordered magnetic state comprising of non-collinear spin arrangement as well as defects, vacancies, stress and broken bonds<sup>15,16,17,18</sup>. Due to the existence of such a magnetically disordered surface layer, magnetic frustration can occur. As a result a cluster glass state may form which causes the bifurcation between FC and ZFC susceptibility curve below  $T_C$ . The origins of the finer features in FC and ZFC curves are not clear at present.

The magnetic field dependence of magnetization for nanoparticles shows ferromagnetic nature even at the lowest temperature 3.3 K (Fig. 3). For both the samples at 225 K and 3.3 K, magnetization does not saturate even at 70 kOe magnetic field (Fig. 3). This type of unsaturated magnetization even in presence of quite high magnetic field for nanoparticles has been observed in some earlier experimental studies<sup>16,21</sup>. Magnetization for 45 nm sample is larger than that in 30 nm for all field values at 225 K. However, at 3.3 K the situation reverses, there magnetization for 30 nm sample is larger than that for 45 nm.

From the magnetization measurements on nanocrystalline samples, no clear evidence of ferromagnetic to antiferromagnetic transition has been observed, but the ferromagnetic transition temperature remains almost same as that of bulk sample. As the particle size is

reduced, the formation of CO state is highly disturbed. The fraction of antiferromagnetic CO state in the nanoparticles may be too small to dominate over the ferromagnetic interaction. As a result, the distinct ferromagnetic to antiferromagnetic transition disappears.

In case of manganite nanoparticle system, the ferromagnetic interaction is governed by the core spins inside the grains. Though the reduction of particle size does not substantially affect the ferromagnetic interaction in case of the nanocrystalline samples, but the existence of the random non-collinear spins as well as the defects, dislocations etc. in the surface layers can reduce the value of magnetization in comparison with the bulk. Magnetic field as high as 70 kOe seems to be not enough to align the surface spins. As a result,  $M(H)$  (at 225 K and 3.3 K) does not saturate (Fig. 3). For the bigger sized particles the surface effect is less than that for the smaller sized particles. Therefore, the susceptibility for 45 nm particle sized sample is larger than that of 30 nm particle sized sample in the temperature range above  $\sim 140$  K (Fig. 2). For the same reason, the value of magnetization in  $M(H)$  at 225 K for 45 nm particles is also larger in comparison with 30 nm particles for all magnetic field value. But in low temperature it appears that the fraction of antiferromagnetic CO state in 45 nm particles slightly dominates over that for 30 nm particles. This is reflected in higher susceptibility value of 30 nm particles in comparison to 45 nm in temperature below  $\sim 140$  K (Fig. 2) and also in  $M(H)$  curve at 3.3 K, where  $M$  for 30 nm sample is larger than 45 nm sample for all magnetic field values (Fig. 3).

The melting of CO state by magnetic field can give rise to large negative MR. The existence of the non-collinear spin arrangements in surface layers can also play vital role in the magnetotransport phenomena. The temperature dependence of resistivity has been studied in the presence of 80 kOe magnetic field for the bulk as well as nanocrystalline samples. Magnetoresistance is defined as  $[R(H) - R(0)]/R(H)$ , where  $R(H)$  is resistance in presence of magnetic field and  $R(0)$  is resistance in absence of magnetic field. For the polycrystalline bulk sample, the variation of negative MR with temperature indicates that there exist a small peak in negative MR at around I-M transition temperature ( $\sim 270$  K) (Fig. 5). The negative MR starts to increase abruptly with decreasing temperature below  $\sim 130$  K which almost coincides with the temperature where zero field resistivity starts to increase sharply with the lowering of temperature as well as the reported charge order transition temperature for the bulk sample<sup>12</sup>. It reaches  $\sim 3000$  % at 3.3 K. This sharp increase of negative MR is due to the melting of CO state by magnetic field. Here we have used the inflationary

definition of MR to clearly indicate the increase of MR with decreasing temperature up to the lowest temperature. The negative MR also increases with the decrease of temperature in the low temperature for both the nanocrystalline samples (Fig. 5). The increase of negative MR is quite gradual. The value of MR at lowest temperature is substantially lower than that obtained for the bulk sample. If we compare the value of negative MR between the two nanocrystalline samples, it appears that the value of MR for the 30 nm particles is larger than that for the other nanoparticle sample above  $\sim 40$  K. Below that temperature the value of MR for bigger sized nanocrystalline sample (45 nm particle sized sample) dominates over that for the smaller sized nanocrystalline sample. The effect of surface layers can also influence the high field magnetoresistance<sup>19,20</sup>. The smaller sized particles having relatively larger surface effect can exhibit larger high field magnetoresistance than the bigger sized particles for the temperatures above  $\sim 40$  K. It seems that the melting of CO fraction by magnetic field in nanoparticles is the major contributor to MR below  $\sim 40$  K. As, the fraction of CO state is larger in bigger sized particles, the value of negative MR is larger for the sample in comparison with the smaller particle sized sample below that temperature. The difference in the fraction of charge ordered antiferromagnetic states in case of two different particle sized samples at low temperature is expected to influence the magnetic field dependence of the magnetoresistance. With this motivation resistivity has been measured as a function of magnetic field at 3.3 K for the two nanocrystalline samples. To highlight the low field magnetoresistance more clearly we have used conservative definition of MR as,  $[R(H) - R(0)]/R(0)$  (%). The variation of MR with magnetic field (0 – 70 kOe) at 3.3 K has been shown in Fig. 6. For both the nanocrystalline samples, there exists faster increase of the value of negative MR at low magnetic field which points out the existence of low field magnetoresistance (LFMR). LFMR, quantified as the value of MR by extrapolating the higher field MR to zero field, is observed to be  $\sim 10\%$  for 30 nm particle. This is larger than that for 45 nm particle for which LFMR is  $\sim 4\%$ . LFMR may originate from domain wall scattering. It has been discussed earlier that the fraction of CO state appears to be larger in 45 nm in comparison to 30 nm particle at 3.3 K. Thus, in case of 30 nm particle the fraction of ferromagnetic state is larger as indicated in fig. 3 [B]. Probably, for this reason, LFMR in this case is also larger than that of 45 nm particle. In higher magnetic field region ( $H > 30$  kOe), the value of MR is higher in 45 nm in comparison to 30 nm particle. The high field MR can be dominated by the melting of CO state. As the fraction of CO state

is larger in 45 nm sample, the value of MR for this sample exceeds the value for 30 nm at high magnetic field.

Though for polycrystalline bulk and nanocrystalline samples, the ferromagnetic ordering temperatures are almost same, metallic state is only achieved in polycrystalline bulk sample (Fig. 1). The fraction of CO state seems to be too small to give distinct antiferromagnetic signature in magnetization. However, resistivity increases with the decrease of temperatures as expected for CO sample. To get the better understanding of transport property, we have performed I-V measurements at different temperatures (Fig. 7). The I-V characteristics are non-linear in nature for all temperatures up to 300 K in case of nanocrystalline samples (Fig. 7). It is reported that for the charge ordered samples, the nonlinearity, hysteresis as well as negative differential resistance (NDR) in I-V can be observed due to the melting of CO state by electric field<sup>22</sup>. But we have not observed hysteresis and NDR in I-V characteristics. In present case nonlinear behavior in I-V is appeared even at 300 K. In case of nanocrystalline materials due to crystalline defects in the grain boundary regions, potential energy barrier may be developed. It will affect the conduction between grain to grain. Electrons have to tunnel through the potential barrier. Due to this tunneling phenomena, I-V characteristics can be non linear in nature. In our nanoparticle system, this strong grain boundary effect plays the key role in transport and causes the suppression of metallic state as well as uprise in resistivity with the decrease of temperature.

#### IV. SUMMARY

To summarize, we have shown that the reduction of grain size largely affects the formation of CO state in case of  $\text{Pr}_{1/2}\text{Sr}_{1/2}\text{MnO}_3$  nanoparticles and the distinct ferromagnetic to antiferromagnetic transition associated with CO transition is not evident. When the grain size is reduced,  $T_C$  does not change appreciably in comparison with the bulk sample but the metallic state disappears and resistivity increases with the lowering of temperature. Through I-V characteristic study, we have argued that this is due to the grain boundary effect in the nanoparticle systems. From the magnetization studies, it appears that the nanocrystalline samples exhibit cluster glass like behavior. The magnetization measurements along with the magnetoresistance measurements also reveal that the small CO fraction may be present at low temperature only and this fraction is larger in 45 nm particles than that of 30 nm

particles.

- 
- <sup>1</sup> *Physics of Manganites*, Ed. T. A. Kaplan and S. D. Malhanti (Kluwer, New York ), 1999.
  - <sup>2</sup> *Colossal Magnetoresistance, Charge ordering and Related Properties of Manganese Oxides*, Ed. C.N.R. Rao and R. Raveau (World Scientific, Singapore, 1998).
  - <sup>3</sup> *Colossal Magnetoresistive Oxides*, Ed. Y. Tokura (Gordon and Breach Science Publishers).
  - <sup>4</sup> H. Kuwahara, Y. Tomioka, a. Asamitsu, Y. Moritomo and Y. Tokura, *Science*, **270**, 961 (1995).
  - <sup>5</sup> E.O. Wollan and W. C. koekler, *Phys. Rev.* **100**, 545 (1955).
  - <sup>6</sup> P. Schiffer, A. P. Ramirez, W. Bao and S-W. Cheong, *Phys. Rev. Lett.*, **75**, 3336 (1995).
  - <sup>7</sup> Z. Jirak, S. Krupika, V. Nekvasil, E. Pollert, G. Villeneuve and F. Zounova, *J. Magn. Magn. Matter.*, **15-18**, 519 (1980).
  - <sup>8</sup> E. Pollert, S. Krupika and E. Kouzmicova, *J. Phys. Chem. Solids.*, **43**, 1137 (1982).
  - <sup>9</sup> Y. Tomioka, A. Asamitsu, H. Kuwahara, Y. Moritomo and Y. Tokura, *Phys. Rev. B*, **53**, R1689 (1996).
  - <sup>10</sup> H. Yoshizawa, R. Kajimoto, H. Kawano, Y. Tomioka and Y. Tokura, *Phys. Rev. B*, **55**, 2729 (1997).
  - <sup>11</sup> K. Knizek, Z. Jirak, E. Pollert, F. Zounova and S. Varatislav, *J. Sol state. Chem.*, **100**, 292 (1992).
  - <sup>12</sup> Y. Tomioka, A. Asamitsu, Y. Moritomo, H. Kuwahara and Y. Tokura, *Phys. Rev. Lett.*, **74**, 5108 (1995).
  - <sup>13</sup> R. Kajimoto, H. Yoshizawa, Y. Tomioka and Y. Tokura, *Phys. Rev. B.*, **66**, 180402(R) (2002).
  - <sup>14</sup> H. Kawano, R. Kajimoto, H. Yoshizawa, Y. Tomioka H. Kuwahara and Y. Tokura, *Phys. Rev. Lett.*, **78**, 4253 (1997).
  - <sup>15</sup> R. H. Kodama, A. E. Berkowitz, E. J. McNiff and S. Foner, *Phys. Rev. Lett.*, **77**, 394 (1996).
  - <sup>16</sup> O. Crisan, M. Angelakeris, N. K. Flevaris and G. Filoti, *J. Optoelectronics and Adv. Materials*, **5**, 959 (2003).
  - <sup>17</sup> J.M.D. Coey, *Phys. Rev. Lett.*, **27**, 1140 (1971).
  - <sup>18</sup> Zhi-Hong Wang, Tian-Hao Ji, Yi-Qian Wang, Xin Chen, Run-Wei Li, Jian-Wang Cai, Ji-Rong Sun and Bao-Gen Shen, *J. Appl. Phys.*, **87**, 5582 (2000).
  - <sup>19</sup> M. Ziese, *Phys. Rev. B* , **60**, R738 (1999).
  - <sup>20</sup> L. Balcells, B. Martinez, F. Sandiumenge and J. Fontcuberta, *J. Magn. Magn. Mat.*, **211**, 193

(2000).

<sup>21</sup> D. Zitoun, M. Respaud, M. Fromen, M. Casanove, P. Lecante, C. Amiens, B. Chaudret, Phys. Rev. Lett., **89**, 037203 (2002).

<sup>22</sup> A. Asamitsu, Y. Tomioka, H. Kuwahara and Y. Tokura, Nature, **388**, 50 (1997).

Fig.1. Resistivity as a function of temperature for 30 nm, 45 nm nanocrystalline and polycrystalline bulk sample of  $\text{Pr}_{1/2}\text{Sr}_{1/2}\text{MnO}_3$ . Inset: temperature dependence of resistivity in high temperature region. I-M transition temperature ( $T_C$ ) and the temperature at which resistivity starts to increase sharply ( $T_{CO}$ ) for the bulk sample are indicated by arrows.

Fig.2. Zero Field Cooled Susceptibility as a function of temperature for 30 nm, 45 nm nanocrystalline and polycrystalline bulk samples of  $\text{Pr}_{1/2}\text{Sr}_{1/2}\text{MnO}_3$ . Measurement has been done in presence of 20 kOe magnetic field.

Fig.3. Magnetization as a function of magnetic field for 30 nm, 45 nm and polycrystalline bulk sample at (A) 225 K and (B) 3.3 K. Inset: Magnetization as a function of field in low magnetic field region.

Fig.4. Zero Field Cooled and Field Cooled Susceptibility as function of temperature for the nanocrystalline sample of particle size 45 nm. Measurement has been performed at 100 Oe magnetic field.

Fig.5. Magnetoresistance  $[\text{R}(\text{H})-\text{R}(0)]/\text{R}(\text{H})$  as a function of temperature for 80 kOe magnetic field. The sharp increase of negative magnetoresistance with decreasing temperature near  $T_{CO}$  for the bulk sample is indicated by arrow. Inset: peak in negative magnetoresistance around the ferromagnetic transition temperature for the bulk sample.

Fig.6. Magnetoresistance as a function of magnetic field for 30nm and 45nm sized nanocrystalline samples at 3.3 K. Magnetoresistance is defined as  $[\text{R}(\text{H})-\text{R}(0)]/\text{R}(0)$ . Inset: Indication of low field magnetoresistance.

Fig.7. I-V Characteristics for nanoparticles: (A) 30 nm (B) 45 nm at 100 K, 200 K and 300 K.

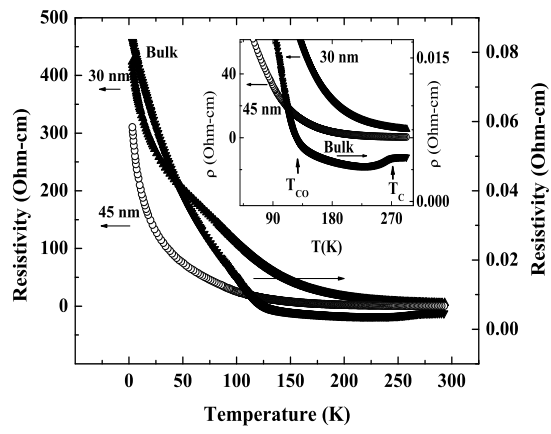


FIG. 1:

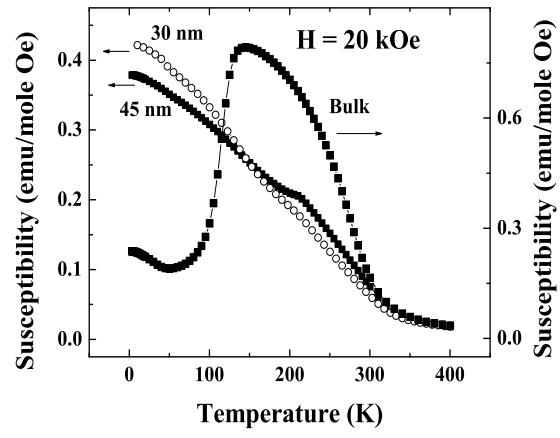


FIG. 2:

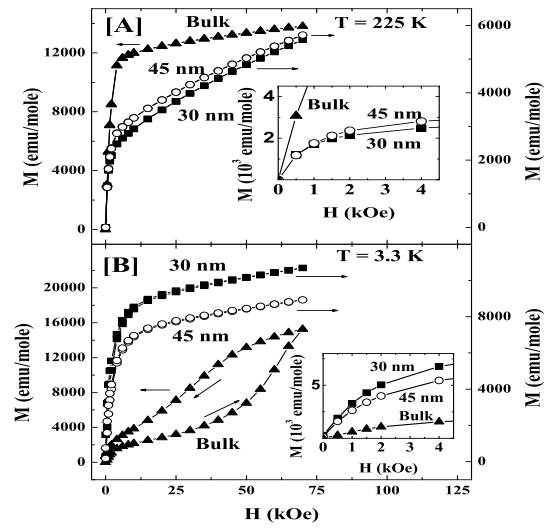


FIG. 3:

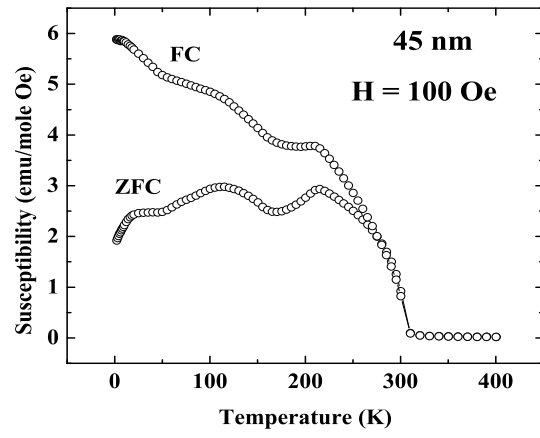


FIG. 4:

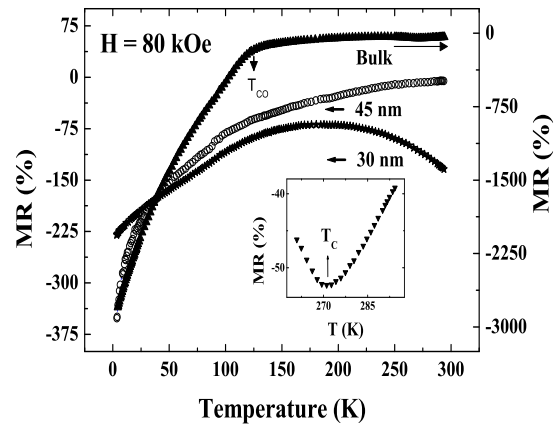


FIG. 5:

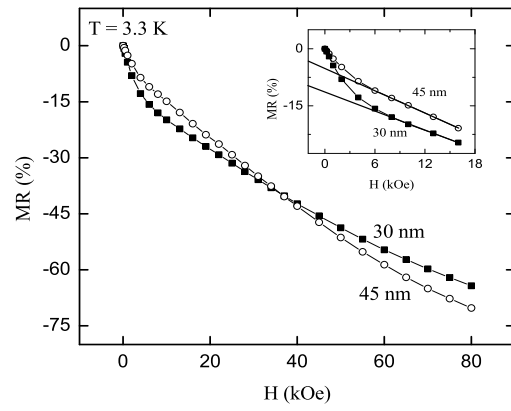


FIG. 6:

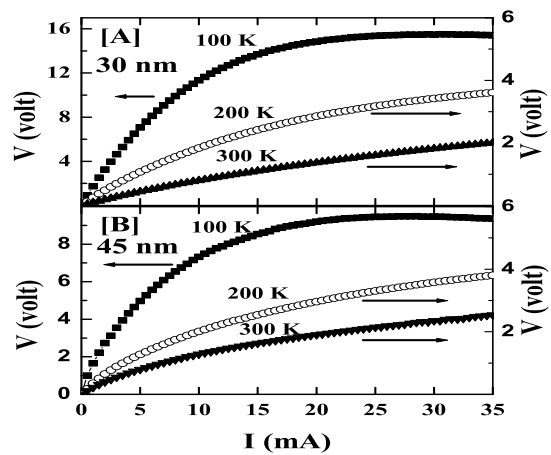


FIG. 7: